Voltage Stability Interface Limits in Non-Uniform Geomagnetic Disturbances

Luke Lowery
Dept. Electrical Engineering
Texas A&M University
College Station, TX USA
lukel@tamu.edu

Adam B. Birchfield
Dept. Electrical Engineering
Texas A&M University
College Station, TX USA
abirchfield@tamu.edu

***Abstract*—Geomagnetic disturbances (GMD) are rare events that threaten grid reliability, where the severity of the impact is highly uncertain. Transformer saturation caused by geomagnetically induced currents (GIC) produce an excess of reactive power loading, capable of decreasing voltage magnitude. Furthermore, traditional interface flow limits regarding voltage stability can become obsolete during a GMD due to these increases. Real time GMD-informed voltage stability limits would provide system operators with valuable information to help with mitigation of extreme solar storm effects. In this paper, the set of possible electric field permutations is searched to find a lower bound on interface stability limits with respect to a base operating condition. The interface limits are discussed as a function of the maximum electric field magnitude produced by a solar storm of a given strength. Numerical analysis techniques are utilized to identify a lower bound on interface flow limits that preserve voltage stability.**

***Index Terms*—Geomagnetic disturbance (GMD), Geomagnetically induced current (GIC), interface flow limits, voltage stability.**

I. Introduction

The impact of geomagnetic disturbances on the power grid arises primarily from the increase of reactive power loads due to half-cycle saturation in transformers. Harmonic signals produced by saturation, in addition to hotpot heating, can cause outages and equipment damage [1] [2] [3]. Despite the research surrounding modeling the impacts of GMDs, much remains unknown regarding how drastically a GMD can impact the operational flexibility of a transmission system.

Physical mitigation techniques such as transformer GIC blocking devices (BDs) can improve local voltage stability by removing the GICs ground path. However, studies indicate that the local improvement may come at the cost of transformers without GIC BDs [4]. Inefficient BD installation may then overwhelm transformers in the region, risking voltage stability issues.

In this paper we attempt to establish a well-defined impact measurement of GMDs on voltage stability. A useful approximation can be calculated by reducing the scope of stability to a single transmission interface - the transaction of active power between a predefined set of buses. This approach to the stability can borrow principles from traditional voltage stability and numerical techniques from continuation power flow. Approximate interface limits can be determined by finding the point of collapse for some known electric field.

However, the electric field of a GMD is not static. It changes, evolves, and can behave erratically where the earth conductance abruptly changes [5] (i.e. coast lines). Locally, the electric field may appear more or less uniform, but on a state or national scale this is no guarantee.

To address this issue, this paper presents a method for computing a conservative upper bound on interface injection when considering voltage stability constraints. Given a GMD capable of producing some maximum electric field, a numeric method is developed to determine conditional interface flow limits deviating from a nominal operating point of the transmission system.

II. Notation

Matrices with a tilde decoration denote a diagonal matrix (i.e. $\tilde{B}$). Vectors take the form of bolded lowercase (i.e. $\mathbf{x}, \eta$). Subscripts denote some attribute of the vector or matrix. Superscripts discriminate between edge and vertex vectors only where strictly necessary (i.e. $\mathbf{x}^\ell, \mathbf{x}^b$). The element counts n_b, n_ℓ, n_x, n_w, n_s, are the number of buses, lines, transformers, windings, and substations, respectively.

III. Background

In order to model GICs, the neutral currents flowing through applicable transformers must be calculated. This portion is a completely linear computation. The resulting reactive power draw of the transformer is often modeled as a constant current proportional to the neutral current. A more thorough derivation in [6] walks the reader through common modeling choices.

A. Conductance Network

The flow of geomagnetically induced currents (GICs) can be calculated using DC circuit analysis techniques as the electric field behaves in a quasi-dc fashion. Network matrices provide an efficient way to compute the DC currents and voltages of the system. Determining if a specific line or winding will contribute to the GICs depending on transformer configurations, substation conductance, etc [7].

The substation grounding conductance diagonal matrix should only consider substations with at least one transformers that does not posses a GIC BD. Let $\mathbf{g}_s \in \mathbb{R}_+^{n_s}$, $\mathbf{g}_w \in \mathbb{R}_+^{n_w}$ and $\mathbf{g}_\ell \in \mathbb{R}_+^{n_\ell}$ be the vectors of substation grounding, winding, and line conductance, respectively.

$$\tilde{G} = \text{diag}\left(\begin{bmatrix}\mathbf{g}_w \\ \mathbf{g}_\ell\end{bmatrix}\right) \quad \tilde{G}_s = \text{diag}\left(\begin{bmatrix}\mathbf{g}_s \\ 0\end{bmatrix}\right)$$

The incidence matrix (1) describing the mapping of lines and transformer windings should only include those that contribute or observe GICs, which is dependent on transformer grounding and configuration [8]. The applicable winding incidence matrix $A_w \in \mathbb{R}^{n_w \times (n_s+n_b)}$ and the line incidence matrix $A_\ell \in \mathbb{R}^{n_\ell \times (n_s+n_b)}$ are concatenated.

$$A = \begin{bmatrix}A_w \\ A_\ell\end{bmatrix} \tag{1}$$

The conductance Laplacian (2) similar to the traditional Y_{bus} matrix, describes the conductance network as impacted by GICs.

$$G = A^T \tilde{G} A + \tilde{G}_s \tag{2}$$

B. Geomagnetically Induced Currents

The induced line voltages caused by the present electric field induce quasi-dc currents into the network. Given some electric field, $\vec{E}$, the induced line voltage is calculated as the contour integral along the path of the line.

$$V_{emf} = \oint \vec{E} \cdot d\vec{\ell}$$

Let $\mathbf{v}_{emf} \in \mathbb{R}^{n_\ell}$ represent the vector of induced dc line voltages. The winding voltages are included in this vector, but their elements should be zero as an induced voltage on a winding will be negligible compared the transmission lines. The Norton equivalent line currents and net nodal Norton currents are calculated before the net line currents can be calculated.

$$\mathbf{i}^\ell_{nort} = \tilde{G}\mathbf{v}_{emf}$$
$$\mathbf{i}^b_{nort} = A^T \mathbf{i}^\ell_{nort}$$

The total line GICs are calculated using Kirchhoff's Current Law, adding induced currents and ground currents. Additionally, the vector is divided by three to obtain the per-phase dc current.

$$G\mathbf{v}^b_{dc} = \mathbf{i}^b_{nort}$$
$$\mathbf{i}_{gic} = (\tilde{G}A\mathbf{v}^b_{dc} - \mathbf{i}^\ell_{nort})/3$$

C. Transformer Saturation and Losses

The permutation matrices $P_x \in \mathbb{R}^{n_b \times n_x}$ and $P_{low}, P_{high} \in \mathbb{R}^{n_x \times (n_w+n_\ell)}$ map transformer currents to a mounted bus, and the low/high winding GICs to their transformers, respectively. Let $\mathbf{n}_t$ be the vector of turns ratios for each transformer

$$\mathbf{n}_t \in \mathbb{R}_+^{n_x} \quad N_t = \text{diag}(\mathbf{n}_t)$$

The effective neutral current of a transformer for auto and grounded transformers is the absolute value of the high and low winding currents by the turns ratio [9]. This value should be put into per-unit.

$$\mathbf{i}_{eff} = \left|(P_{high} + N_t^{-1} P_{low})\mathbf{i}_{gic}\right|$$

Choice of load the modeling function $f_{loss} : \mathbf{i}_{eff} \mapsto \mathbf{q}_{loss}$ is subject to discretion. This paper uses a constant-reactive current scalar function (3) for demonstrative purposes. It will be shown that if the losses monotonically increase w.r.t neutral current magnitude, the methods used will hold.

Let $\mathbf{k} \in \mathbb{R}_+^{n_x}$ be the vector of transformer constants in per-unit and let $K = \text{diag}(\mathbf{k})$ its respective diagonal matrix. Finally, let $\mathbf{v} \in \mathbb{R}^{n_b}$ be the vector of ac bus voltage magnitudes.

$$f_{loss}(\mathbf{i}_{eff}) = \mathbf{v} \cdot K\mathbf{i}_{eff} \tag{3}$$

Matrix H maps induced line voltages to effective transformer neutral currents.

$$H = (P_{high} + N_t^{-1} P_{low})(\tilde{G}AG^{-1}A^T\tilde{G} - \tilde{G})/3$$

Since K is a positive-definite matrix the matrix $H^{'} = KH$ is merged for utility in analysis. The final form of reactive power losses contributed by GICs (4) is computed with 2 matrix operations and an absolute value operator, where $H^{'}$ embeds the network's GIC characterization.

$$\mathbf{q}_{loss} = \mathbf{v} \cdot P_x \left|H^{'}\mathbf{v}_{emf}\right| \tag{4}$$

IV. Static Storm Interface Limits

In the context of this paper, an *interface* shall be defined by two sets of buses. The first set will increase its effective bus generation, while the second set will decrease effective generation. Let the vector $\eta \in \mathbb{R}^{n_b}$ define this interface. Positive and negative elements of η represent increase in supply and demand buses, respectively. The elements are restricted to (5) to denote a balanced change in generation dispatch.

$$\sum \eta_+ = 1 \qquad \sum \eta_- = -1 \tag{5}$$

The span of the vector, $\alpha\eta$, represents the size of the injection across the defined interface. The power flow mismatch equations (6) including transformer GIC losses are modified to include transformer GICs and the interface injection.

$$\begin{aligned} f_p &= g_p(\mathbf{p}_g, \mathbf{p}_d, \mathbf{v}, \theta) - \alpha\eta \\ f_q &= g_q(\mathbf{q}_g, \mathbf{q}_d, \mathbf{v}, \theta) + \mathbf{v} \cdot \mathbf{i} \end{aligned} \tag{6}$$

Where the ac network constraints g_p, g_q include the active and reactive generation and demand, $\mathbf{p}_g, \mathbf{p}_d, \mathbf{q}_g, \mathbf{q}_d$ and voltage magnitude and angle, $\mathbf{v}, \theta$. The introduced Γ function (7) determines the largest value of α, representing the maximum possible interface injection.

$$\begin{aligned} &\Gamma(\eta, \mathbf{i}) = \max(\alpha) \\ &\text{subject to} \quad \begin{cases} \alpha \in \mathbb{R} \\ 0 = g_p(\mathbf{p}_g, \mathbf{p}_d, \mathbf{v}, \theta) - \alpha\eta \\ 0 = g_q(\mathbf{q}_g, \mathbf{q}_d, \mathbf{v}, \theta) + \mathbf{v} \cdot \mathbf{i} \\ \mathbf{q}_{g,min} \le \mathbf{q}_g \le \mathbf{q}_{g,max} \end{cases} \end{aligned} \tag{7}$$

The implementation of this function is a modified version of the continuation power flow [10]. The constraint on injection can be either (a) voltage magnitude limits or (b) bifurcation.

This paper will consider bifurcation as the injection maximum. The following analysis is only slightly modified if some minimum bus voltage constrains the injection instead.

V. GMD Minimum Interface Limit

Ascertaining the set of electric field orientations that *minimize* the interface stability limit will approximate a safe upper bound on interface flow. This is an approximation because it assumes that the only deviation from the base case is through the interface injection. Maintaining the interface below the limit can provide operational guidelines during a GMD of some known strength.

A. The Set of Transformer Neutral Currents

Assume that for a given GMD, some maximum observable electric field magnitude $|\vec{E}|$ can be determined for each line in the system. The range of possible induced line voltages then has an upper and lower bound, induced by direct alignment of the electric field (8). Let the vector $\mathbf{e}_{max} \in \mathbb{R}_+^{n_\ell}$ define $|\vec{E}|$ line maximums in volts-per-kilometer and the diagonal matrix $L \in \mathbb{R}_+^{n_\ell \times n_\ell}$ define lengths of each line in kilometers. It should be noted that not all of the electric fields defined by this set are necessarily plausible configurations.

$$V = \{\mathbf{v} \in \mathbb{R}^{n_\ell} | -\tilde{L}\mathbf{e}_{max} \leq \mathbf{v} \leq \tilde{L}\mathbf{e}_{max}\} \tag{8}$$

The set I_{eff} is defined as the set of possible constant reactive current transformer loads induced by V.

$$I_{eff} = \{\mathbf{i} \in \mathbb{R}_+^{n_x} \mid \mathbf{i} = \left|H^{'}\mathbf{v}\right|, \ \mathbf{v} \in V\} \tag{9}$$

B. Minimum Interface Flow

The function $\Pi : \eta, \mathbf{e}_{max} \mapsto \alpha$ (10) is defined to represent the lowest injection of real power across an interface η that causes voltage-instability given an electric field bound by $\mathbf{e}_{max}$.

$$\begin{aligned} \Pi(\eta, \mathbf{e}_{max}) = \min_{\mathbf{i}} \Gamma(\eta, \mathbf{i}) \\ \text{s.t.} \quad \mathbf{i} \in I_{eff} \end{aligned} \tag{10}$$

It will be assumed moving forward that a strict increase in transformer GICs necessarily causes a decrease in interface transmission capacity.

$$\mathbf{i}^{'} \geq \mathbf{i}$$
$$\Gamma(\eta, \mathbf{i}^{'}) \leq \Gamma(\eta, \mathbf{i})$$

or equivalently $\nabla\Gamma \leq 0$.

The sensitivities of Γ are desired so that the changes in $\mathbf{i}$ decrease Γ via gradient descent. Notably, Γ is non-linear due to the power flow constraint. Consider the differentiation of the constraints of Γ, where η and $\mathbf{i}$ are treated as differential variables.

$$\begin{aligned} d\Gamma &= \eta_0^T d\eta \\ 0 &= \frac{\partial f_p}{\partial \theta} d\theta + \frac{\partial f_p}{\partial \mathbf{v}} d\mathbf{v} - d\eta \\ 0 &= \frac{\partial f_q}{\partial \theta} d\theta + \frac{\partial f_q}{\partial \mathbf{v}} d\mathbf{v} + \tilde{V} d\mathbf{i} \end{aligned}$$

At the power boundary, there exists one and only one set of voltages that satisfy the power flow equations. Therefore, any deviation in voltage magnitude or angle will increase bus mismatch. A numerically stable direction in the voltage space is chosen, $d\theta = 0$, and the boundary sensitivities are computed in the null space of the voltage magnitude.

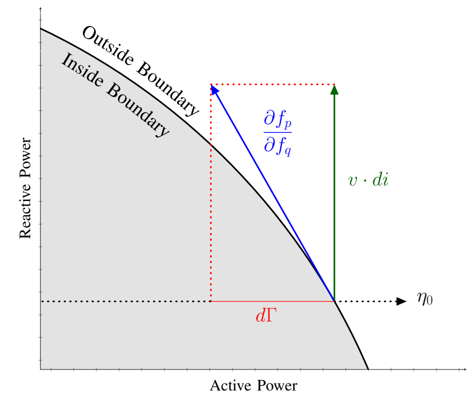

Fig. 1. Sensitivities of injection vector maximum with respect to constant reactive current loads at the power boundary.

The total derivative (11) measures the sensitivity of Γ as the transformer GICs are infinitesimally increased. Fig. 1 visualizes the relationship between an increase in transformer current loads and the impact on the interface flow magnitude.

$$\frac{d\Gamma}{d\mathbf{i}} = -\eta_0^T \frac{\partial f_p}{\partial \mathbf{v}} \left(\frac{\partial f_q}{\partial \mathbf{v}}\right)^{-1} \tilde{V} \tag{11}$$

VI. Modified Pre-Selection

A. The Domain of Π

Understanding the properties of the set I_{eff} will allow an efficient evaluation of the minimum injection limit. It can be shown that I_{eff} is *star-convex*, which eliminates certain elements of the set from consideration.

Consider (9) and recall that the set of possible line voltages V is convex by observation. As linear transformations of convex spaces preserve convexity, the set transformation $H^{'}V$ is convex. The absolute value operator is effectively a series of reflections and rotations mapping each quadrant to the first quadrant. Since $0 \in H^{'}\mathbf{v}_{emf}$, the absolute value transforms the convex space into a star-shaped space at the zero vector. The union of convex sets that all contain the same point, is star-convex at that point [11].

While gradient descent is capable of improving the objective function locally within a star-convex set, gradient descent tends to fail in most cases [12]. Due to this shortcoming, the primary search method will utilize simplex-like methods of optimization, and transition to gradient descent where accuracy is desired.

B. GIC Current Maximums

A *corner* of this convex space is defined as an element of V where each element of the vector is at the maximum observable magnitude. Prior to acknowledging implausible and non-unique members, there are 2^{n_ℓ} elements in V_{corner}.

$$V_{corner} = \{\mathbf{v} \in V \mid \forall v_k \in \mathbf{v} \quad v_k = \pm \ell_k e_{max,k}\}$$

Then (12) is the subset of I_{eff} mapped by V_{corner}. Let $\rho \in \mathbb{R}^{n_\ell}$ denote a vector whose elements $\rho_i \in \{1, -1\}$ determine the polarity of the aligned electric field at that line.

$$I_{corner} = \{\left|H^{'}\tilde{L}\tilde{E}\rho\right| : \ \rho_i \in \{1, -1\}, \ \rho \in \mathbb{R}^{n_\ell}\} \tag{12}$$

where $\tilde{E} = \text{diag}(\mathbf{e}_{max})$ is the diagonal matrix of local line magnitude maximums. Note that not every element of this set is on the exterior of I_{eff}, but every exterior corner of I_{eff} is in this set.

The set I_{eff} should then be reduced to be as small as possible so that each member maps back to a realistic permutation of the electric field. Disqualifying corners are not limited to:

- Series and parallel lines must always share the same polarity.
- Negation of ρ does not produce a unique solution.
- For a GIC-irrelevant line k, $\forall \rho, \ \rho_k = 0$

Recall that the $\nabla \Gamma < 0$ and that I_{eff} is a star-convex set. If the minimizing value is on the face of I_{eff}, it must be a convex combination of the exterior-mapping corners that share a polarity prior to the absolute value operation. Searching this space would be ineffective due to the high computation time of power flow.

Therefore, the search space will be limited to the set I_{corner} with an understanding that if a face is the minimizing value, there exists a corner that approximates the solution within acceptable tolerance.

C. Linear Greedy Algorithm

The number of elements in I_{corner} increases exponentially with respect to the number of lines in the system. Additionally, multiple iterations of power flow are required to evaluate Γ once. A realistic evaluation of Π then requires a pre-processing algorithm so that only likely candidates are considered.

A high negative correlation exists between the interface flow limit $\Gamma(\eta, \mathbf{i})$ and the total transformer q-current loads of the system, $\Sigma \mathbf{i}$. This property should be leveraged when considering the set of possible minimizing values.

Due to rigid faces of I_{eff}, it is impossible for an edge or face value to produce more total transformer GICs than a corner. The algorithm will only consider corners of the input space due to this observation. This does not, however, imply that an edge value cannot produce more reactive power losses.

Step 1: Begin with polarity vector ρ_0 equal to the sign of a row of H

Step 2: Calculate $\mathbf{i} = \left|H^{'}\tilde{L}\tilde{E}\rho_0\right|$ for every adjacent corner. Signs for parallel and series lines should observe the same change.

Step 3: If a neighboring corner has higher total transformer GICs than ρ_0, switch to that corner and repeat Step 2.

Step 4: If the total GICs of ρ_0 are larger than all neighbors, save the value and repeat Step 1 with a different row of H.

Step 5: Continue until the corner with the maximum transformer GICs is identified.

In a case model that has upwards of hundreds of buses, the top 5 percent of corners that produce the most transformer GICs should be considered for full evaluation. As the number of system elements increases, the correlation coefficient between the interface limit and and total transformer GICs will inevitably decline. It becomes increasingly plausible that a corner exists that has less system losses yet produces a lower stability bound on a given interface.

VII. Case Study

The 20-Bus GIC test case [13] provides a useful domain to demonstrate the numerical analysis. After generating the H matrix and eliminating redundant mappings, there are approximately 2000 permutations remaining that need a direct evaluation of Γ. The electric field that maximally reduces the stability limits can then be compared to the algorithm's predicted electric field.

The injection vector η_0 will denote an increase in active generation on buses 18 and 19, and a decrease in active generation on buses 7 and 8 as seen in Fig. 2.

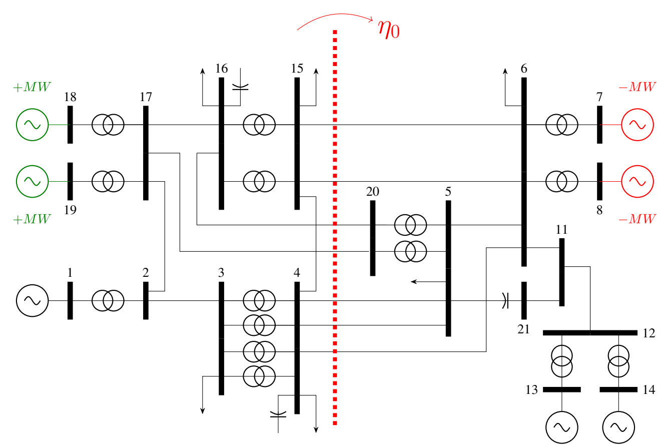

Fig. 2. 20-Bus GIC Case One-line Diagram showing the active power injection interface.

A. The Set of Constant Current Loads

The complete set of possible transformer GICs I_{eff} is difficult to visualize due to the high number of dimensions. Therefore, two-dimensional projections are utilized that show the shadow of the hyper-shape. The set of possible effective transformer GICs are shown between two transformers prior to absolute value for visualization purposes (Fig. 3). The fractal-like pattern sits within a convex hull that is defined by a set of edges, should they be shown.

The shadow represents the relationship of the possible transformer GICs produced by a GMD between two transformers. Most notably, parallel transformers experience next to no

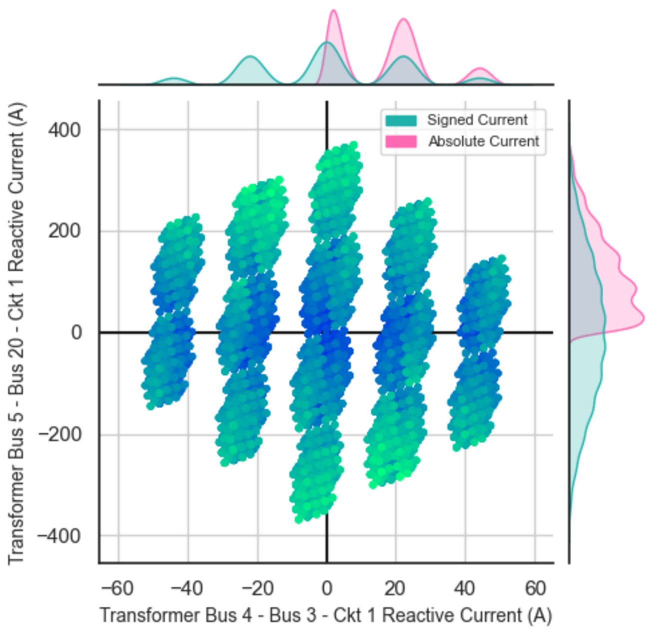

Fig. 3. Lower dimensional projection of the set of possible transformer constant reactive current loads as the joint distribution of two transformers. Green data points indicate more total transformer GICs.

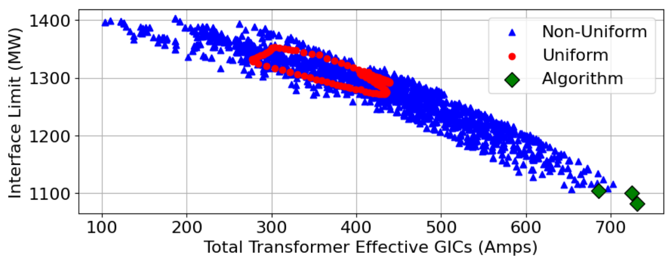

Fig. 4. Interface Injection limit plotted against the total transformer effective currents at $\mathbf{e}_{max} = 2$ volts-per-kilometer. The set of uniform storms at the set magnitude are plotted with the corners of the non-uniform storms to compare their respective restrictions on the injection vector. The algorithm's predictions are plotted on top of the set of non-uniform corners in green.

deviation from their proportional relationship. This means that regardless of GMD strength, parallel transformers will observe similar relative impact through saturation, all else being equal.

B. Limiting Electric Field

The most limiting non-uniform electric field severely diminishes the interface compared to any uniform electric field (Fig. 4). Interestingly, the vector field associated with this solution is one of the most plausible permutations (Fig. 5). The electric field is pointing in the general northward direction, deviating only in the east and west direction. Most of the corners observe a strong curl in the vector field.

The electric field of crossing transmission lines at the point of overlap cannot have the electric field in two separate directions. This is equivalent to a singularity in the electric field, which was not considered in the omission stage of the plausible voltage permutations.

C. Algorithm Performance

For every $\mathbf{e}_{max}$ calculated, the algorithm successfully converged to the minimizing solution. This implies that the minimizing corner is the same regardless of the maximum electric field magnitude. The convergence progress (Fig. 6) reaches three local maximum, two of which are the two most minimizing electric field configurations.

There is significance to the initial guesses matching the signs of rows of H. Each initial guess represents the polarities that cause the highest possible currents for that row's respective transformer. Converging to the electric field permutation that has the largest total transformer GICs is certain from at least one of these starting vectors - given the geometry of the search space.

D. Variation in Storm Magnitude

The most imposing electric field function, $\Pi(\eta_0, \mathbf{e}_{max})$, is evaluated over a range of electric field magnitudes. The interface limits imposed by varying maximum electric field magnitudes (Fig. 7) has a roughly linear relationship.

The strong decreasing trend suggests that the assumed relationship between total transformer GICs and most imposing electric field permutation holds true.

VIII. Discussion and Conclusion

The results of the paper provide a promising method of establishing stability reassurances during a GMD. This method could be extended to larger cases in future work, for instance the east-west interface of the Texas interconnect where stability is a concern [14]. Additionally, the algorithm can be improved through probabilistic weightings of the electric field, discriminating by either region or latitude.

Accurately modelling the non-linear saturation losses in the transformers would also provide an immediate improvement to the algorithm's accuracy, potentially at the loss of computation time depending on the model.

The analysis and case study of this paper demonstrated a successful approach to determine a lower bound to interface stability as a function of the maximum observable electric field magnitude. The discovered the relationship between the total transformer GICs and the interface limit was effectively leveraged against the size of the input space. Relaxing the non-linear optimization problem to a related linear maximization problem accelerated the optimization problem the 20-bus GIC case. The continuation of this work will focus on understanding the limitations of this relation, especially in the context of case size.

If correctly implemented for practical use operation, this GMD-informed voltage stability metric would provide valuable information in preparation and response to solar storms. Future research should focus on methods of computing indicators and approximations for the relationship between saturation losses and its impacts on a given interface. A fast, reliable

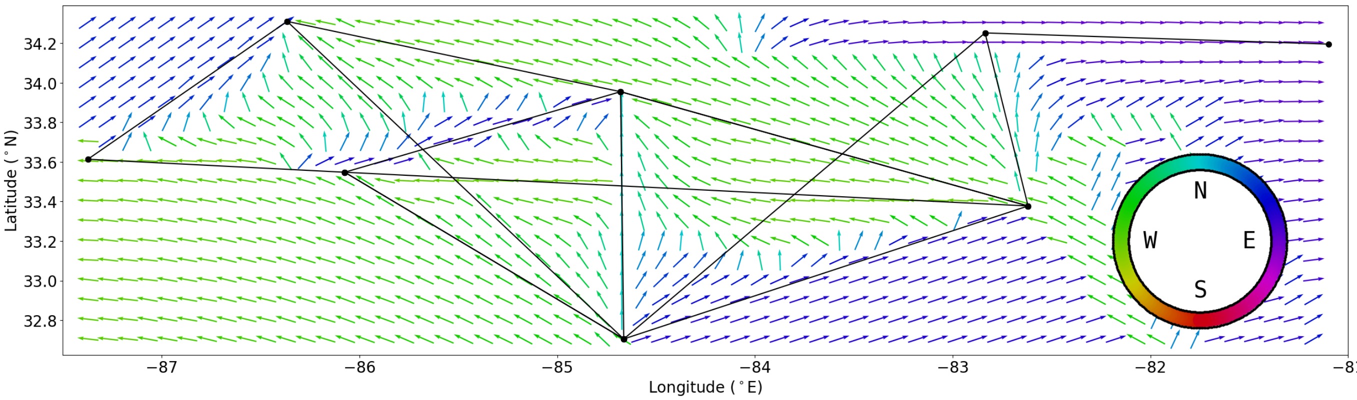

Fig. 5. Spatial interpolation of the electric field permutation that minimizes the interface η_0 injection limit. The electric field is aligned with each circuit except for those that do not contribute to GICs. The color wheel indicates the cardinal direction of the electric field as an aid.

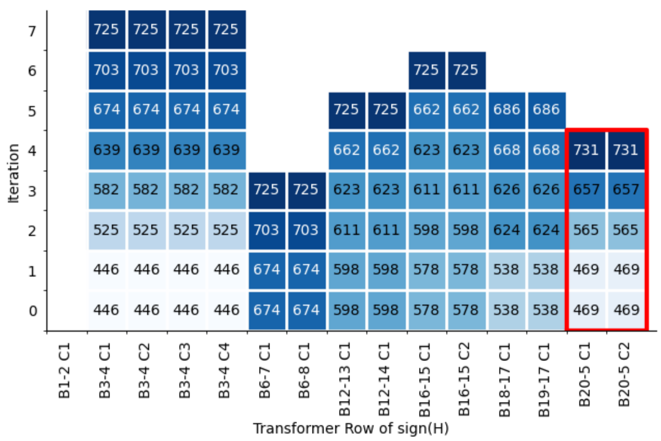

Fig. 6. Greedy algorithm convergence plot. The x-axis represents the initial polarity vectors, each of which is associated with a transformer row in H. The height of each column shows the number of iterations until a local maximum was reached. Cell values are equal to the total transformer GICs at $\mathbf{e}_{max} = 2$, and red-boxed columns converged to the minimizing solution.

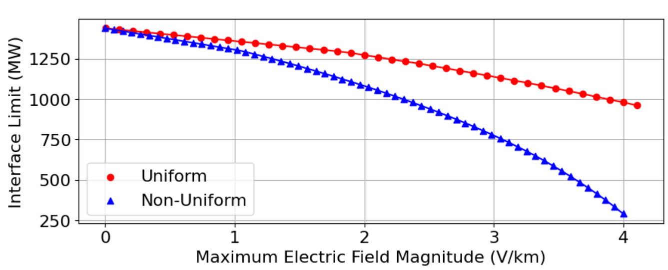

Fig. 7. The minimum stable injection limit plotted against the maximum observable electric field magnitude. Uniform electric field is plotted for comparison.

way to set interface limits to ensure voltage stability would provide a numerically justified system response to ongoing and predicted GMDs.

ACKNOWLEDGMENTS

Support is gratefully acknowledged from the U.S. Department of Energy, Office of Cybersecurity, Energy Security, and Emergency Response (DOE-CESER), Award Number 38601.

REFERENCES

[1] R. Girgis and K. Vedante, "Effects of gic on power transformers and power systems," in *PES TD 2012*, pp. 1–8, 2012.

[2] Z. M. K. Abda, N. F. A. Aziz, M. Z. A. A. Kadir, and Z. A. Rhazali, "A review of geomagnetically induced current effects on electrical power system: Principles and theory," *IEEE Access*, vol. 8, pp. 200237–200258, 2020.

[3] J. Ramírez-Niño, C. Haro-Hernández, J. H. Rodriguez-Rodriguez, and R. Mijarez, "Core saturation effects of geomagnetic induced currents in power transformers," *Journal of Applied Research and Technology*, vol. 14, no. 2, pp. 87–92, 2016.

[4] H. Zhu and T. J. Overbye, "Blocking device placement for mitigating the effects of geomagnetically induced currents," *IEEE Transactions on Power Systems*, vol. 30, no. 4, pp. 2081–2089, 2015.

[5] X. Wang and S. Zhang, "The geoelectric field coast effect: Results from two dimensional finite element method and analytic solutions," *Alexandria Engineering Journal*, vol. 77, pp. 525–536, 2023.

[6] T. J. Overbye, T. R. Hutchins, K. Shetye, J. Weber, and S. Dahman, "Integration of geomagnetic disturbance modeling into the power flow: A methodology for large-scale system studies," in *2012 North American Power Symposium (NAPS)*, pp. 1–7, 2012.

[7] D. Boteler and R. Pirjola, "Modelling geomagnetically induced currents," *Space Weather*, vol. 15, 12 2016.

[8] T. Divett, G. Richardson, C. Beggan, C. Rodger, D. Boteler, M. Ingham, D. Mac Manus, A. Thomson, and M. Dalzell, "Transformer-level modeling of geomagnetically induced currents in new zealand's south island," *Space Weather*, vol. 16, 05 2018.

[9] Y. Si, Z. Wang, and L. Liu, "Sensitivity analysis of power system small signal stability to geomagnetic disturbances," *International Journal of Electrical Power Energy Systems*, vol. 148, p. 108970, 2023.

[10] V. Ajjarapu and C. Christy, "The continuation power flow: a tool for steady state voltage stability analysis," *IEEE Transactions on Power Systems*, vol. 7, no. 1, pp. 416–423, 1992.

[11] A. Rubinov and E. Sharikov, "Star-shaped separability with applications," *Journal of Convex Analysis*, vol. 13, 01 2006.

[12] J. C. Lee and P. Valiant, "Optimizing star-convex functions," in *2016 IEEE 57th Annual Symposium on Foundations of Computer Science (FOCS)*, pp. 603–614, 2016.

[13] R. Horton, D. Boteler, T. J. Overbye, R. Pirjola, and R. C. Dugan, "A test case for the calculation of geomagnetically induced currents," *IEEE Transactions on Power Delivery*, vol. 27, no. 4, pp. 2368–2373, 2012.

[14] S. C. Johnson, J. D. Rhodes, and M. E. Webber, "Understanding the impact of non-synchronous wind and solar generation on grid stability and identifying mitigation pathways," *Applied Energy*, vol. 262, p. 114492, 2020.